Hindawi
Wireless Communications and Mobile Computing
Volume 2022, Article ID 2453144, 7 pages
https://doi.org/10.1155/2022/2453144

Research Article

Application of Cable Climbing Robot Automation Control Technology in Bridge Cable Measuring System

Weihua Zhou,[1] **Junqi Bao**,[2] **Zhenzhi Liu**,[2] **and Zhengda Chen**[2]

[1]*College of Electrical Engineering, Zhejiang University, Hangzhou 318000, China*
[2]*Hangzhou Changchuan Technology Co., Ltd., Hangzhou 310056, China*

Correspondence should be addressed to Weihua Zhou; dididi@zju.edu.cn

Received 30 September 2021; Accepted 4 December 2021; Published 26 February 2022

Academic Editor: Deepak Gupta

According to the traditional bridge cable measurement system, the accuracy of the bridge cable measurement is low, and the measurement time is long. Based on the automatic control technology of the climbing robot, a new bridge cable measurement system is designed. We design system hardware through CIS drive circuit, main controller, and communication module; design system software on the basis of hardware design; obtain the motion control equation of orthogonal joint cable climbing robot through DH transformation; and apply this equation to the bridge cable measurement system. The bridge cable measurement model is constructed, and the bridge cable measurement system design is completed through the system hardware design and software design. The simulation results show that the designed system has higher accuracy in measuring bridge cables and shorter measuring time.

1. Introduction

As a new type of bridges, cable-stayed bridges are being used more and more in actual production. They have beautiful appearance, relatively low cost, and good seismic resistance. With the continuous improvement of design theories, the continuous updating of materials, the widespread use of electronic computers, the continuous accumulation of construction experience, and the continuous improvement of construction technology, the span of cable-stayed bridges is also increasing, which also indicates that cable-stayed bridges will play an increasingly important role in the future bridge construction [1]. The main force-bearing component of a cable-stayed bridge is a cable, but it is exposed to the atmosphere for a long time and is corroded by wind, sun, rain, and environmental pollution, and its surface will be severely damaged. The main load-bearing part of the bridge is about 25%–30% of the cost of the whole bridge. The damage of the cable surface means that the safety of the cable-stayed bridge will be greatly affected [2]. In order to reduce the loss caused by the uncertain damage of the cable, it is necessary to carry out internal and external measurement, painting, or repair of the cable regularly to improve the safety and image of the bridge [3]. The cable-stayed bridge is mainly composed of a bridge tower under pressure, a cable under tension, and a beam body under bending. In its normal operation, the stay cable will be repeatedly affected by the dynamic load of the bridge deck, wind and rain vibration, sunshine, and corrosive gas, and it is prone to damage to the outer sheath and local steel wire corrosion. The damage of the stay cable sheath causes the internal steel wire to be exposed to the air, and the oil stains attached to the surface of the stay cable may penetrate into the cable, accelerating the corrosion of the steel wire. If it is not regularly maintained, this will eventually lead to the failure of the steel wire corrosion and lead to accidents such as cable failure or even bridge deck collapse. As the main load-bearing structure of cable-stayed bridges and suspension bridges, the effective metal bearing area of the cable is directly related to the safety and service life of the bridge, so it is necessary to

measure the bridge cable. In order to ensure the accuracy of the measurement and the safety of the personnel, the automation technology of the bridge cable measurement is now being studied at home and abroad [4].

Literature [5] designed a long-distance monitoring system for bridge cable force based on LoRa; designed a low-power, low-collision star-shaped wireless network structure using LoRa wireless communication technology; introduced the principle of measuring cable force by vibration frequency method; gave the overall structure and modular design of the monitoring system; and finally carried out the cable force monitoring test experiment. The experimental results show that the developed cable force remote monitoring system has perfect functions and strong real-time performance, which provides an efficient and convenient implementation method for remote and long-term bridge monitoring and has a relatively broad application prospects. However, the bridge cable measurement accuracy of this system is low. Cui proposed a cable-stayed bridge cable anchoring measurement system based on data transmission [6]. Based on the establishment of bridge construction control network and main tower linear monitoring, certain technical means were used to transfer plane coordinate datum and elevation coordinate datum to the main tower. For the construction section, according to the accuracy requirements of the measurement location and the conditions of the instrument's visibility, the absolute station method of the total station, the relative station method, or the method of combining the total station and the vertical cast point is selected to realize the rapid and high construction of the cable anchor system [6]. Yi et al. designed an ultrasonic testing system for axial force of cable clamp screw of suspension bridge [7]. First, the ultrasonic probe was fixed on one end of the screw to excite the ultrasonic wave. The ultrasonic wave propagated in the screw shaft along the axial direction to the other end surface to be reflected. The ultrasonic probe received the reflected wave and then used it. The software system measured the change in ultrasonic echo sound to obtain the screw axial force. After the system was tested and the coefficient was calibrated, the system was applied to the cable clamp screw axial force detection of the Wuhan Yangsigang Yangtze River Bridge. The results show that the system has good performance. The reliability of the test is about 3.5% under the condition that the stress-free echo sound is clear. The test of the single screw axial force in the Wuhan Yangsigang Yangtze River Bridge screw test took less than 1 min [7]. Real bridge detection is convenient and quick. However, the bridge cable measurement time of the last two systems is long.

In order to solve the defects of low measurement accuracy and long time of traditional bridge cable measurement system, an automatic control technology of cable climbing robot based on bridge cable measurement system is designed, and the effectiveness of the system is verified by simulation experiments. This method can be applied to the regular measurement of bridge cables. Through the rapid and accurate detection of bridge cables, the risk factors can be found in time to maintain the safety of the bridge.

2. Design of Bridge Cable Measurement System Based on Automatic Control Technology of Cable Climbing Robot

2.1. System Hardware Design. The hardware design part of the bridge cable measurement system includes the CIS drive circuit, the main controller, and the communication module.

2.1.1. CIS Drive Circuit. The driving circuit of CIS mainly includes the provision of CIS working clock (CLK) and start pulse (SP). The recommended operating clock frequency of the linear solid-state image sensor SV200A4-10 is 250 kHz, and the duty cycle is 25%–50%. If the clock frequency is too high or the duty cycle is too large, the integration time of the photosensitive element integration circuit will be reduced, and the output signal amplitude of the CIS will be too small. Under the excitation of the start pulse, the CIS starts a frame of scanning, and the width of the start pulse must be at least not less than one working clock. The clock signal (CLK) and the start pulse signal (SP) of the CIS can be generated by the timer of the DSP by dividing the frequency of the internal clock or can be provided by an external programmable logic device or other circuits. In the system, in order to reduce the complexity of the circuit, the drive signal of the CIS is provided by the multifunction serial port of the DSP [8].

TMS320C32 is equipped with a serial port, which can send and receive 8-bit, 16-bit, 24-bit, and 32-bit data in both directions by setting the registers. In the continuous working mode, it can continuously send and receive any number of words without the need for a new synchronization pulse. TMS320C32 provides eight memory-mapped control registers to control serial port operations. They include an overall control register, two port control registers, three transmit/receive timer registers, one data receiving buffer register, and one sending buffer register [9]. Among them, the overall control register is used to control the overall function of the serial port and determine the operation mode of the serial port; the two port control registers are used to control the functions of the six serial ports; the transmit buffer is used to buffer the next word to be sent; and the receive buffer is used to buffer the last received word. The TMS320C32 serial port has a strong load capacity. Its sending clock pin CLKX and sending frame synchronization pin FSX can directly drive the CIS without any bus enhancement circuit. The interface circuit is very simple. The connection diagram of DSP and CIS is shown in Figure 1.

2.1.2. Main Controller. The function of the main controller is as follows: the wireless serial port communicates with the host computer, connects to the CAN bus, and then processes the large amount of data fed back. In order to facilitate the realization of these two points, when designing the master controller, combined with the characteristics of the slave controller, this article selects STM32F103, which can fully meet these functional requirements. STMicroelectronics STM32 series chips are based on the ARM Cortex-M3 core

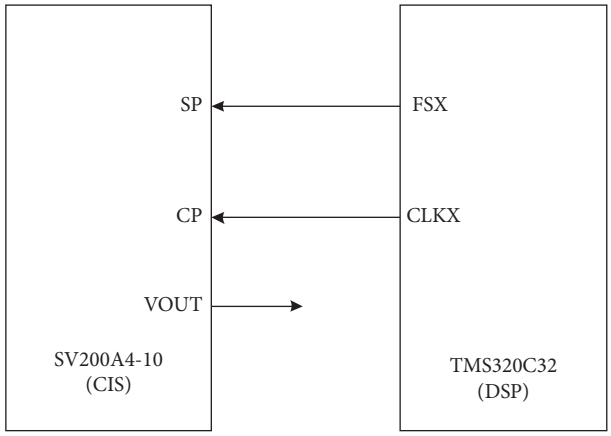

Figure 1: Connection diagram between DSP and CIS.

and are cost-effective 32-bit processors that can meet the needs of high-performance, low-cost, and low-power embedded applications [10].

The STM32F103 selected in this article belongs to the "enhanced" series of STM32, with a clock frequency of 72 MHz. The specific model of the prototype developed in this article is the STM32F103C8T6 main controller with 64 KB of flash storage space, 20 KB of SRAM space, and seven timers. The timer of the MCU can generate 30 PWM outputs and up to 9 communication interfaces. The specific performance is shown in Table 1. The package has a small size and good versatility, which is convenient for the development of the main controller used in this article.

The design block diagram of the main controller is shown in Figure 2. Its volume requirement is very small, so the design is compact. The power supply of the whole controller is 1A low dropout voltage stabilizer AMS1117. The stable output voltage is 3.3 V. The main controller is in low-level reset mode and can be freely selected in JTAG or SWD mode, which is convenient for software code writing and debugging [11].

2.1.3. Communication Module. The communication mainly includes the communication between the ground PC and the master controller and the communication between the master and slave controllers in the prototype. The ground PC communicates with the main controller through the 2.4 G wireless communication module, the prototype body adopts master-slave distributed control, and the main controller communicates with the slave controllers through the CAN bus [12]. The communication topology is shown in Figure 3.

(1) Ground PC to the main controller: the wireless communication between the ground PC and the main controller is realized through the 2.4 G wireless serial port module. An RS232-TTL converter is connected to the DB9 serial port of the PC to realize the full-duplex TTL of the physical layer. In asynchronous serial communication, the data link layer is a commonly used duplex 8N1 (8 data bits, no parity, 1 stop bit) serial frame with a baud rate of 9600, and the main controller interrupts the receiving wireless serial port. The information is bridged with the CAN bus, and at the same time, its own information and the sensor information obtained on the bus are sent back to the ground PC through the wireless serial port to realize status monitoring [13].

(2) Master controller to slave controller: due to the mechanical size of the robot body, the CAN node circuit should avoid complexity, and the circuit board size should be as small as possible. Therefore, the on-chip integrated CAN controller can be efficiently processed with the minimum CPU load. The STM32F103 series processors with a large number of received messages are used as MCUs. The physical layer is the topological structure of the CAN bus, and the data link layer is a half-duplex message that can be framed, arbitrated, acknowledged, and calibrated at a rate of 1 Mbps. Its function is in the hardware of the CAN controller. At the same time, the software sets CAN parameters (working mode, baud rate, filter), sends message requests, processes message reception, manages interruptions, and obtains

Table 1: Specific parameters of STM32F103C8T6.

Series to which IC belongs	STM32 F1
Core processor	ARM® Cortex™-M3
Core size	32 bits
Speed	72 MHz
Connectivity	CAN, I^2C, IrDA, LIN, SPI, UART/USART, USB
Peripheral equipment	DMA, PWM, PDR, POR, PVD, PWM, temperature sensor, WDT
Number of inputs/outputs	37
Program memory capacity	64 KB (64 K × 8)
Program memory type	Flash memory
RAM capacity	20 K × 8
Voltage-power (Vcc/Vdd)	2 V~3.6 V
Data converter	A/D 2 × 10 × 12b
Oscillator type	Internal
Operating temperature	−40°C~85°C
Encapsulation/shell	48-LQFP

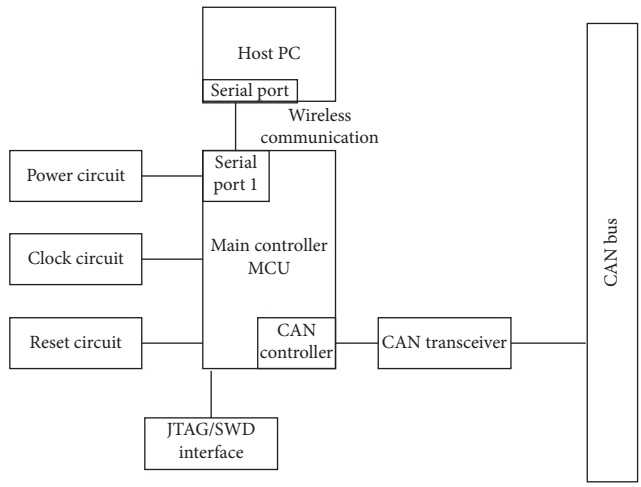

Figure 2: Design block diagram of the main controller.

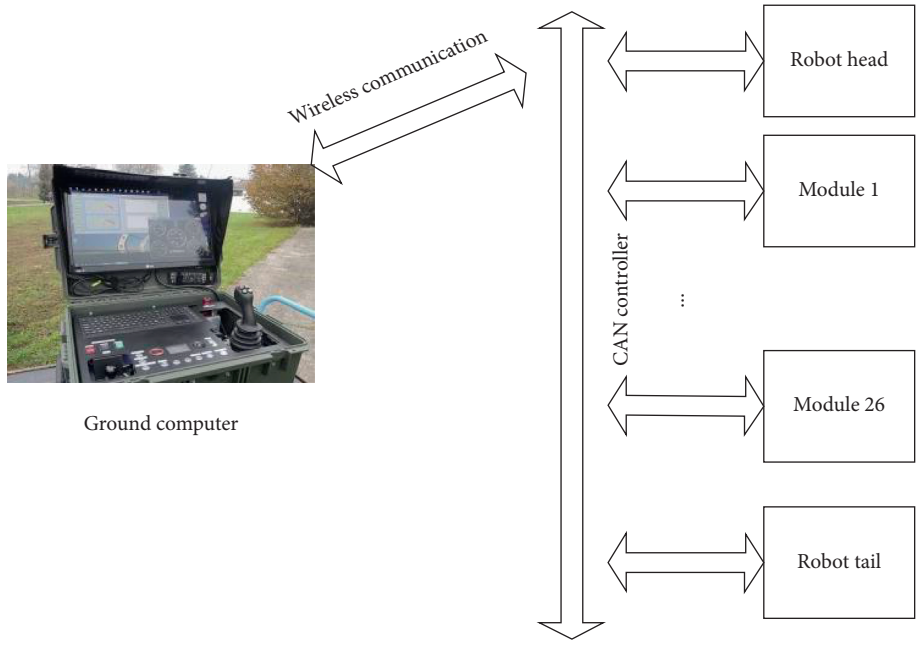

Figure 3: Communication topology.

diagnostic information through registers such as status, control, and configuration [14].

2.2. System Software Design. Because the rope climbing robot is similar to a biological snake without limbs and wheels, the force when it moves comes from the friction between the surface of its body and the contact object (e.g., ground). The rotation of the module joints inside the body will cause the friction of all parts of the body. The magnitude and direction of the force are different, and the imbalance of the force produces a movement trend, forming various movement patterns. The rope climbing robot can imitate the movement of some biological snakes and create a movement pattern that biological snakes do not have [15]. At present, the prototypes of cable climbing robots made by domestic and foreign scholars can move in two-dimensional space, and some even made attempts to move in three-dimensional space. The basic motion modes of the rope climbing robot are meandering motion, traveling wave motion, side shifting motion, and rolling motion. Winding motion, traveling wave motion, and lateral motion are all imitating the motion patterns of biological snakes, and traveling wave motion can be understood as a meandering motion in the vertical direction [16]. In order to obtain the spatial pose (position and posture) of the joint points of each module of the cable climbing robot, it is necessary to perform kinematics modeling for its high-redundancy system [17]. Because the cable climbing robot prototype in this paper adopts a serial modular structure, Denavit–Hartenberg transformation can be used to establish the kinematics model of the cable climbing robot through the simplified spatial linkage model. In the kinematics analysis of joint robots, the DH matrix is the most widely used. First, a coordinate system is fixed on each link of the robot, and then a homogeneous transformation matrix is used to represent the relative poses of two adjacent links. The multiplication transformation can finally derive the pose of the end joint point relative to the base coordinate system, thereby establishing the kinematics equation of the robot [18].

In this paper, the motion control equation of the orthogonal joint cable climbing robot can be obtained through DH transformation, and the bridge cable can be measured according to this equation. We use the DH transformation to establish the DH coordinate system for the prototype of the cable climbing robot with the modular structure in series, establish the base coordinate system $O_0X_0Y_0Z_0$ near the head of the robot, and take the center of the rotation axis of the joint (steering gear) in each module as the origin $O_1, O_2, \ldots, O_n$ of each coordinate system. Z_i axis is set as the rotation axis of each steering gear, looking from the head end to the end, which follows the body axis and rotates counterclockwise around it. X_i axis is set as the male perpendicular of the Z_i axis, looking from the steering gear i to the steering gear $i + 1$, of which the direction is set as the positive direction of the X_i-axis. The Y_i-axis is determined by the right-hand screw rule. The link DH coordinate system of the rope climbing robot is shown in Figure 4.

According to the establishment of the DH coordinate system of the rope climbing robot, the DH matrix of each module can be obtained as

$$T_i = \begin{bmatrix} s\theta_i & c\theta_i & 0 & 0 \\ c\theta_i & -s\theta_i & 0 & L_0 \\ 0 & 0 & 1 & 0 \\ 0 & 0 & 0 & 1 \end{bmatrix}. \quad (1)$$

In the formula, L_0 is the distance between the joint axis of the first module and the base coordinate system, 3 cm; L is

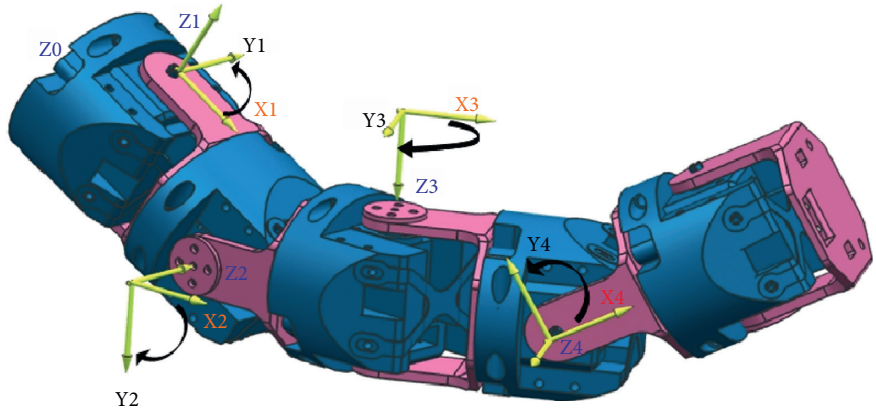

Figure 4: Link DH coordinate system of rope climbing robot.

the length of the module, 7 cm; and θ_i is the rotation angle of each steering gear in the module. The transformation matrix of the module can be obtained by multiplying the DH matrices of first i ${}^0T_i$ and the space position of the i-th module can be obtained from the space coordinate by T_i, so the space position of each module can be obtained, and the kinematics model of the climbing robot can be established as

$$T_1 = P_0 \cdot {}^0T_i. \tag{2}$$

In the formula, P_0 is the homogeneous coordinate of the head end of the rope climbing robot in the base marking system, which can be at the origin of the base marking system or in other positions. Therefore, the space coordinate of the i-th module is $P_i(X_iY_iZ_i)$; when P_0 and θ_i are known, the spatial configuration of the rope climbing robot can be obtained.

The robot part of the prototype in this paper is composed of orthogonally connected modules. According to the connection characteristics, they can be divided into two groups: pitch modules and yaw modules. The rotation axis of the pitch module and the rotation axis of the yaw module are perpendicular to each other. In the initial state, the rotation axes of all pitch modules are parallel to the horizontal plane, and the rotation axes of all yaw modules are perpendicular to the horizontal plane. If the rope climbing robot rotates around its body axis by $0 \pm 90^\circ$, the pitch module and the yaw module swap positions. If the first module is a yaw module, the second and even-numbered modules are both pitch modules, and the odd-numbered modules are yaw modules. The motion control equation of the orthogonal joint cable climbing robot is

$$E_i = A_i \cdot \mathrm{SIN}(w \cdot t + k \cdot t) + \gamma_i. \tag{3}$$

In the formula, i represents the module number, A_i represents the maximum rotation angle of the i-th module, w represents the frequency of the module angle change, k represents the motion control parameter, and γ_i represents the angle compensation amount.

We apply the motion control equation of the orthogonal joint cable climbing robot to the bridge cable measurement system to construct the bridge cable measurement model:

$$Q_i = \frac{E_i}{T_1 L}. \tag{4}$$

3. Simulation Experiment Analysis

3.1. Introduction to Experimental Environment. In order to verify the application of the cable climbing robot automation control technology in the cable measurement system, firstly, the simulation environment of the cable climbing robot is established using the Webots mobile robot simulation software, and the simulation platform is built according to the prototype in a 1 : 1 ratio. The i7 is simulated and tested in a computer with 5600U@2.6 GHz, memory 8GB1600MHz.

Webots is professional multifunctional mobile robot simulation software that integrates modeling, programming, simulation, and program migration developed by the Swiss Federal Institute of Technology. Based on VRML (virtual reality language), the modeling environment of robots is more convenient for its development. At present, nearly 400 universities and research institutions at home and abroad have applied Webots series software to carry out related research on robot technology. Webots software is based on OpenGL technology with a built-in 3D compiler, which can perform 3D modeling of the operating environment and robots. The scene tree is used to display the properties of objects in the simulation environment. The parameters can be edited in combination with the model. The code area is the code of the controller. The code area is the code of the controller, which supports programming language supports C/C++, Python, Java, and other IDEs, such as visual studio. The console displays debugging information and controller output parameters. Webots provides a wealth of sensor and driver models. The available sensors include cameras, distance sensors, light sensors, position and force sensors, and GPS. It provides humanoid robots, simulated robots, mobile robots, and connecting rod joints. The research and development of robots facilitate the learning and application of the platform. The simulation cable climbing robot built in the Webots environment is shown in Figure 5.

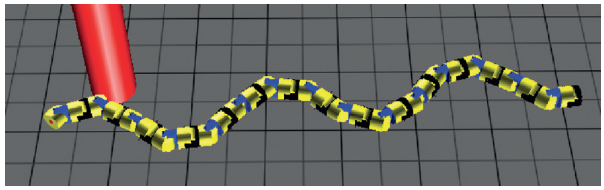

Figure 5: A simulation platform of a rope climbing robot based on Webots.

The entire rope climbing robot is composed of 30 orthogonal 30 modules, which are driven by Servo. The motion control of the robot in the simulation environment is to assign values to the Servo parameters at each moment, and different rotation angles have different motion modes for the rope climbing robot. First, click controller in the general node in the scene tree, select the associated controller code file, click "Edit" to enter the code writing interface, then call the necessary precompiled header files, and set and initialize the relevant values; in the control program by obtaining keyboard commands to dynamically select the motion mode, Servo rotates the angle calculated by the control equation with time as a function to perform the simulation.

3.2. Comparison of Measurement Accuracy of Different Systems. Under the above-mentioned simulation platform, the bridge cable measurement system based on cable climbing robot automatic control technology designed in this paper, the cable-stayed bridge cable anchor measurement system based on datum transfer designed in literature [6], and the suspension bridge cable clamp designed in literature [7] are adopted. The screw axial force ultrasonic testing system measures the bridge cables to verify the measurement accuracy of the three systems. The comparison results are shown in Figure 6.

According to Figure 6, it can be seen that the cable measurement accuracy of the cable climbing robot automatic control technology designed in this paper is up to 99%, which is better than the cable-stayed bridge cable anchor measurement system based on datum transfer designed in [6], and [7] designed the suspension bridge cable clamp screw axial force ultrasonic testing system to measure the bridge cable with high accuracy.

3.3. Comparison of Measurement Time of Different Systems. Using the bridge cable measurement system designed in this paper based on the automatic control technology of the climbing robot, the cable-stayed bridge cable anchor measurement system based on datum transfer designed in literature [6], and the ultrasonic testing system of the screw axial force of the suspension bridge cable clamp designed in literature [7], a comparative analysis of the bridge cable measurement time was conducted, the comparison result is shown in Table 2.

According to the analysis in Table 2, the shortest measurement time of cable-stayed bridge cable anchor measurement system designed in [6] is 240.7 s, the shortest measurement time of suspension bridge cable clamp screw

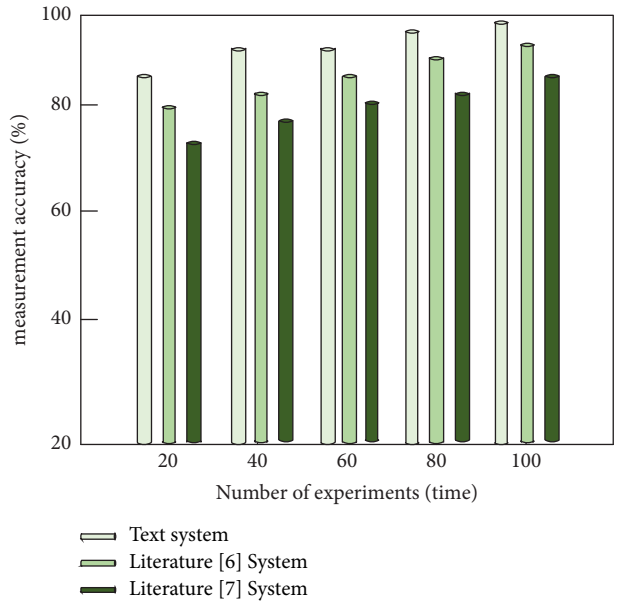

Figure 6: Comparison results of the bridge cable measurement accuracy of the three systems.

Table 2: Comparison results of bridge cable measurement time of different systems.

Number of experiments/time	Average bridge cable measurement time (s)		
	Text system	Literature [6] system	Literature [7] system
10	541.8	550.7	556.5
20	458.5	510.5	540.7
30	401.6	485.6	498.5
40	387.7	420.4	405.2
50	312.0	398.0	351.6
60	247.2	374.8	298.7
70	198.4	320.2	255.1
80	102.9	291.6	196.3
90	105.7	240.7	152.0
100	124.0	340.4	275.1

axial force ultrasonic detection system designed in [7] is 152.0 s, and the shortest measurement time of bridge cable measurement system designed in this paper based on cable climbing robot automatic control technology is 102.9 s. This shows that the bridge cable measurement system based on the automatic control technology of cable climbing robot designed in this paper takes a short time in cable measurement, has good performance, and can achieve the purpose of design.

4. Conclusion

With the rapid development of society, bridges have become an indispensable part of modern transportation. As the key load-bearing structure of cable-stayed bridge and suspension bridge, the effective metal bearing area of cable is directly related to the safety and service life of the bridge. Aiming at remedying the shortcomings of low measurement accuracy and long time of traditional bridge cable

measurement system, a new bridge cable measurement system based on automatic control technology of climbing robot is designed in this paper. The CIS driving circuit, main controller, and communication module in the hardware are designed; the motion control equation of the orthogonal joint cable climbing robot is obtained by calculating the DH transformation; the bridge cable measurement model is constructed; and the design of the new bridge cable measurement system is completed. By comparing this system with two traditional systems for simulation experiments, it is concluded that the cable measurement accuracy of the system designed in this paper is as high as 99% and the shortest measurement time is 102.9 s, which verifies the effectiveness of the system, achieves the purpose of system design in this paper, brings significant social and economic benefits, and lays a good foundation for bridge engineering in our country.

Data Availability

The datasets used and/or analyzed during the current study are available from the corresponding author on reasonable request.

Conflicts of Interest

The authors declare that there are no conflicts of interest.

References

[1] Y. B. Liang, S. J. Cai, and Q. Feng, "The PE appearance detection technology of the bridge cables of Wuhan Tianxingzhou Yangtze River Bridge based on drone aerial photography," *Geodesy and Geodynamics*, vol. 39, no. 11, pp. 1207–1210, 2019.

[2] Y. P. Ou, J. G. Shi, and J. Zhang, "Design and realization of anthropomorphic climbing robot based on single chip microcomputer," *Industrial Technology Innovation*, vol. 40, no. 5, pp. 42–49, 2020.

[3] M. L. Che, "Application design of remote control in measuring robot," *Electronic World*, vol. 15, pp. 177-178, 2019.

[4] X. Liu, "Application of intelligent control technology in the field of industrial robot control," *Technological Innovation and Application*, vol. 10, no. 15, pp. 177-178, 2020.

[5] L. X. Wu and Y. G. Sun, "Design of remote monitoring system for bridge cable force based on lora," *Software*, vol. 41, no. 1, pp. 216–219, 2020.

[6] W. Cui, "Cable-stayed bridge cable anchor measurement technology based on datum transfer," *Modern Surveying and Mapping*, vol. 42, no. 1, pp. 57–59, 2019.

[7] J. J. Yi, X. M. Peng, and B. Wang, "Ultrasonic testing technology for axial force of suspension bridge cable clamp screw," *Bridge Construction*, vol. 49, no. z1, pp. 68–73, 2019.

[8] H. Welch and S. Mondal, "Analysis of magnetic wheel adhesion force for climbing robot," *Journal of Mechatronics and Robotics*, vol. 3, no. 1, pp. 534–541, 2019.

[9] D. Cruz-Ortiz, M. Ballesteros-Escamilla, I. Chairez, and A. Luviano, "Output second-order sliding-mode control for a gecko biomimetic climbing robot," *Journal of Bionics Engineering*, vol. 16, no. 4, pp. 633–646, 2019.

[10] P. Zhao, M. T. Wu, and J. X. Gu, "Design and production of a climbing robot for climbing rope," *Electronic Design Engineering*, vol. 26, no. 23, pp. 121–129, 2018.

[11] S. Yu, C. Ye, G. Tao, J. Ding, and Y. Wang, "Design and analysis of a modular rope-climbing robot with the finger-wheeled mechanism," *Journal of Mechanical Science and Technology*, vol. 35, no. 5, pp. 2197–2207, 2021.

[12] D. N. Badodkar and T. A. Dwarakanath, "Machines, mechanism and robotics, lecture notes in mechanical engineering," in *Proceedings of the iNaCoMM 2017, Design and Analysis of Spring-Based Rope Climbing Robot*, pp. 453–462, Springer, Berlin, Germany, 2019.

[13] S. Yoo, I. Joo, J. Hong, J. Kim, H. S. Kim, and T. Seo, "Mechanical and empirical parameter design on a multi-wound differential pulley winch for a wall-climbing robot," *International Journal of Precision Engineering and Manufacturing*, vol. 21, no. 5, pp. 857–867, 2020.

[14] R. S. Bisht, P. M. Pathak, and S. K. Panigrahi, "Experimental investigations on permanent magnet based wheel mechanism for safe navigation of climbing robot," *Procedia Computer Science*, vol. 133, pp. 377–384, 2018.

[15] H. J. Zhuang, J. Li, and W. Wang, "Research on power tower climbing robot system," *Automation & Instrumentation*, vol. 246, no. 4, pp. 205–210, 2020.

[16] C. C. Yan, H. H. Zhang, and H. Han, "Design and implementation of intelligent climbing robot based on single chip microcomputer," *Science and Technology Information*, vol. 17, no. 7, p. 2, 2019.

[17] Y. J. Lv, L. T. Wang, and F. Su, "Design and kinematic model simulation of XY-DELTA redundant robot," *Machine Tool & Hydraulics*, vol. 489, no. 15, pp. 77–80, 2019.

[18] P. Li, X. Duan, G. Sun, X. Li, Y. Zhou, and Y. Liu, "Design and control of a climbing robot for inspection of high mast lighting," *Assembly Automation*, vol. 39, no. 1, pp. 77–85, 2019.